Heart, Lung and Circulation (2017) xx, 1–9
1443-9506/04/$36.00
http://dx.doi.org/10.1016/j.hlc.2017.05.138

ORIGINAL ARTICLE

Absence of Myostatin Improves Cardiac Function Following Myocardial Infarction

Sarina Lim, MBChB, FRACP, MD [a*], Chris D. McMahon, PhD [b], Kenneth G. Matthews, PhD [b], Gerard P. Devlin, MBChB, FRACP, MD [a], Marianne S. Elston, MBChB, FRACP, PhD [a], John V. Conaglen, MBChB, FRACP, MD [a]

[a]Waikato Clinical Campus, Faculty of Medical and Health Sciences, University of Auckland, New Zealand
[b]Developmental Biology Group, AgResearch Limited, Hamilton, New Zealand

Received 27 March 2017; received in revised form 20 May 2017; accepted 24 May 2017; online published-ahead-of-print xxx

Background Myostatin inhibits the development of skeletal muscle and regulates the proliferation of skeletal muscle fibroblasts. However, the role of myostatin in regulating cardiac muscle or myofibroblasts, specifically in acute myocardial infarction (MI), is less clear. This study sought to determine whether absence of myostatin altered left ventricular function post-MI.

Methods Myostatin-null mice ($Mstn^{-/-}$) and wild-type (WT) mice underwent ligation of the left anterior descending artery to induce MI. Left ventricular function was measured at baseline, days 1 and 28 post-MI. Immunohistochemistry and immunofluorescence were obtained at day 28 for cellular proliferation, collagen deposition, and myofibroblastic activity.

Results Whilst left ventricular function at baseline and size of infarct were similar, significant differences in favour of $Mstn^{-/-}$ compared to WT mice post-MI include a greater recovery of ejection fraction ($61.8 \pm 1.1\%$ vs $57.1 \pm 2.3\%$, $p < 0.01$), less collagen deposition ($41.9 \pm 2.8\%$ vs $54.7 \pm 3.4\%$, $p < 0.05$), and lower mortality (0 vs. 20%, $p < 0.05$). There was no difference in the number of BrdU positive cells, percentage of apoptotic cardiomyocytes, or size of cardiomyocytes post-MI between WT and $Mstn^{-/-}$ mice.

Conclusions Absence of myostatin potentially protects the function of the heart post-MI with improved survival, possibly by limiting extent of fibrosis.

Keywords Myostatin • Myocardial infarction • Ejection fraction • Fibrosis

Introduction

Myostatin is known to be a negative regulator of skeletal muscle mass [1]. Although myostatin was discovered nearly two decades ago, its role in the heart remains controversial. The expression of myostatin in the heart (protein, mRNA or both) is up-regulated both in rat models of volume-overload, and in patients with congestive heart failure [2–5]. Myostatin also regulates the proliferation of normal and dystrophic skeletal muscle fibroblasts [6,7] and may be an important mediator between cardiomyocytes and fibroblasts, an effect consistent with the activities of other members of the TGF-β superfamily [8]. Therefore, myostatin may play a role in regulating both the viable myocardium and the extent of connective tissue deposition following myocardial infarction (MI).

The aim of this study was to assess if there was a difference in left ventricular function post-MI in the absence of myostatin when compared to controls.

*Corresponding author at: 92 Balmoral Street, Hornsby NSW 2077, Australia. Phone: +612 9987 1588; Fax: +612 9477 1672., Email: sarinalim@cli-nes.com.au

Please cite this article in press as: Lim S, et al. Absence of Myostatin Improves Cardiac Function Following Myocardial Infarction. Heart, Lung and Circulation (2017), http://dx.doi.org/10.1016/j.hlc.2017.05.138

Materials and Methods

Heterozygote $Mstn^{+/-}$ mice (C57BL/6 background) were kindly gifted by Se-Jin Lee, John Hopkins University [1]. Mice were genotyped and bred to homozygosity at the Ruakura Small Animal Colony Unit. Adult male (12-week-old) $Mstn^{-/-}$ and WT (C57BL/6) mice were randomised to induction of MI or sham-control group (n = 12 per genotype and procedure). All animals and surgical procedures were performed with local ethical approval and conformed with the NIH Guidelines for the care and use of laboratory animals.

Induction of MI

General anaesthesia was achieved using a combination of Ketamine, Xylazine and Acepromazine. Mice were intubated and ventilated in a supine position on a 37 °C heated pad. A 10 mm left thoracotomy was performed at the fourth intercostal space and ligation of the LAD artery was made midway between the left atrium and apex of the left ventricle [9]. Successful ligation was attained when blanching of the distal myocardium was observed. Assisted ventilation was maintained until spontaneous breathing was restored. For sham-control, a left thoracotomy was performed without coronary artery ligation. Mice were observed daily in a small animal colony unit with provision of standard chow and water *ad libitum*.

Echocardiogram and Clinical Parameters

Total body weight (BWT) was recorded at baseline and weekly, thereafter. Heart rate (HR) and blood pressure were measured on conscious mice during daylight at baseline, and at day 28 post-surgery using a computerised blood pressure tail-cuff analysis system (Visitech Systems, Apex, NZ, USA). Each measurement was obtained from an average of 25 readings.

Transthoracic echocardiography was performed at baseline, days 1 and 28 post-surgery, using a Philips HDI 5000 Sono CT ultrasound, with a 10 MHz broadband compact linear array transducer (Phillips NZ Ltd, Auckland, New Zealand). Mice were lightly anaesthetised with the aforementioned anaesthetic combination. Imaging was obtained in the parasternal short axis view at the level of the papillary muscle using two-dimensional (2D) and M-Mode analysis [10]. Left ventricular end diastolic and systolic diameters (LVEDD and LVESD respectively) were measured and fractional shortening (FS) and ejection fraction (EF) calculated. Three readings were obtained for each measurement and then averaged. The operator was blinded to the surgical procedure.

Histological Examination

On day 28, the mice were weighed and sacrificed with carbon dioxide asphyxiation, coupled with cervical dislocation. Hearts were rapidly excised, weighed, formalin-fixed and embedded in paraffin wax. Seven micrometre sections were cut longitudinally in the centre of the infarct, and stained with haematoxylin and eosin (H&E). Each section was photographed (Leica DMI6000 B inverted microscope, Leica Microsystems, Germany). The size of the infarct was calculated as previously described [11] using Image J Software (NIH).

Collagen deposition was assessed with Van Gieson staining. A modified grid-counting system was used to estimate the amount of collagen deposition in the peri-infarct region, where viable cardiomyocytes were still present [12]. A grid of equal spaces was created over the region of interest (ie. infarcted and peri-infarcted areas) on each section of the myocardium. Grids that had over 50% of infarcted scar tissue (stained red) were graded as 1, while grids with over 50% of viable tissue (stained yellow/light brown) interspersed with collagen were graded as 2. Grids with only viable cardiomyocytes were not counted as this represents the distant non-infarcted myocardium. The amount of collagen deposition was calculated as a percentage of the infarcted scar tissue to the total region of interest (infarcted + viable).

Immunohistochemistry (IHC)

Immunohistochemistry was performed to: assess DNA synthesis [anti-5-Bromo-2′-deoxyuridine (BrdU)], quantify the size of cardiomyocytes (laminin); and assess apoptosis, programmed necrosis and survival [anti-cleaved caspase-3 (1:300) (#9664, Cell Signalling Technology, MA, USA), anti-PARP-1 (1:10,000) (#1835238, Roche Diagnostics NZ Ltd, Auckland, NZ), anti-$pAkt^{s473}$ (1:100) (#4058, Cell Signalling Technology, MA, USA), anti-$pAkt1/2/3^{s473}$ (1:2000) (SC-7985, Santa Cruz Biotechnology, CA, USA) and anti-$pAkt1/2/3^{t308}$ (1:1000) (SC-16646, Santa Cruz Biotechnology, CA, USA). All were performed according to the manufacturer's protocol. For negative controls, a mouse IgG1 antibody (Dako, # x0931, VWR, Auckland, New Zealand) was used at the same dilution as the primary antibody of interest.

BrdU (0.1 ml/10 g BWT) was injected intra-peritoneally two hours before euthanasia (Cell Proliferation kit, # RPN20, GE Healthcare Life Sciences, Auckland, New Zealand). The total labelling fraction was calculated as a ratio of the BrdU positive cells to the total number of cells counted on each field with six fields per section in the border region of the infarcted ventricle randomly selected [13]. For sham animals, the six fields were randomly taken throughout the left ventricle.

Cells were stained with laminin (Dako, #Z0097, VWR, Auckland, New Zealand) to highlight the cell membrane and counterstained with haematoxylin to visualise the nuclei. A point-counting system was used where a grid of equal spacing was overlaid onto the section. Only cells with well-defined cell membrane and visible nuclei that sit on the 'crosses' of the grid were selected. The minimal Feret diameter and the cross-sectional area were measured from at least 300 consecutive cells in each section using image J (NIH) software.

The immunointensity of the other cellular markers was obtained semi-quantitatively using a multiplicative quick

Please cite this article in press as: Lim S, et al. Absence of Myostatin Improves Cardiac Function Following Myocardial Infarction. Heart, Lung and Circulation (2017), http://dx.doi.org/10.1016/j.hlc.2017.05.138

score method [14]. Briefly, the analysis takes into account both the proportion of positive cells (category A and scored from 1 to 6) and the intensity of the staining (category B, and scored 0 to 3). A quick score is derived from the product of both categories.

Immunofluorescence (IF)

An indirect immunofluorescence method was adopted to localise myofibroblasts using α-smooth muscle actin antibody (α-SMA) at a dilution of 1:100 and overnight incubation (SC-32251, Santa Cruz Biotechnology). This antibody is specific for α-smooth muscle actin, expressed in myofibroblasts and vascular smooth muscle cells but is non-reactive with actin from fibroblasts, myocardium and striated muscle. The number of myofibroblasts was calculated using the grid-counting system as described, where grids with immunofluorescence positivity (orange/red) graded as 1, and grids with only DAPI (blue) was graded as 2. The number of myofibroblasts was estimated as a percentage of positive immunofluorescence to the total immunofluorescence activity (Grade 1 + 2). Grids with blood vessels were excluded from the analysis.

Statistical Analysis

Data were subjected to analysis of variance (ANOVA) using the statistical software package Genstat (release 15.0). Factors of genotype ($Mstn^{-/-}$ or WT), treatment (sham or ligation of LAD) and their interaction were included in the treatment term. Data were logarithmically transformed when required, to stabilise the variance and a geometric mean was derived. All data were presented as mean ± standard error of the mean (SEM). Data were considered to be statistically significant when $p < 0.05$.

Results

Infarct Size Was Similar Between the Two Genotypes

Ligating the LAD artery midway between the left atrial appendage and the apex produced an infarct size of approximately 11% of the left ventricle ($Mstn^{-/-}$ 9.9 ± 1.9% vs WT 12.5 ± 1.8%, $p = 0.38$). No difference was observed between the genotypes. The mean time to complete ligation of the LAD artery was similar between the two groups (29.8 ± 1.4 min vs 27.8 ± 1.0 min respectively, $p = 0.24$). Histopathological examinations of the cardiac tissue at 28 days post-MI revealed an area of ischaemia, and replacement of cardiomyocytes by inflammatory cells and scar tissue. No histological abnormalities were seen in sham-operated mice in which the architecture of the myocardium was preserved (Figure 1).

Absence of Myostatin is Associated With an Improved Survival Post-surgery

Six WT mice died within a few hours following surgery, requiring recruitment of an additional six mice. Of these mice, five died post-MI, while one died in the sham-operated group. The mortality rate was higher in WT compared with $Mstn^{-/-}$ mice (20% vs 0%, $p < 0.05$).

Clinical Parameters

$Mstn^{-/-}$ mice were consistently larger than WT counterparts and remained so throughout the study period. Induction of a myocardial injury did not alter BWT of the $Mstn^{-/-}$ mice over the 28-day period post-MI. Conversely, an almost 7% increase in BWT was observed in WT mice at the end of the study period, irrespective of whether the mice were assigned to the sham or ligation groups ($p < 0.001$).

Baseline resting HR was higher in the $Mstn^{-/-}$ group compared with WT littermates (575.5 ± 11.3 bpm vs 535.9 ± 12.0 bpm, $p < 0.05$), while the opposite was observed at day 28 post-surgery (599.1 ± 12.0 bpm vs 645.4 ± 6.5 bpm, $p < 0.01$), irrespective of surgical procedures. The MAP was significantly greater in WT mice both at baseline and at day 28 post-MI compared with $Mstn^{-/-}$ mice. Induction of MI resulted in a 9% reduction of MAP in the $Mstn^{-/-}$ mice, whilst an increase of almost 6% in MAP was seen in the WT ligation group ($p < 0.05$) (Figure 2).

Restoration of Cardiac Function Post-MI Was Observed in the Absence of Myostatin

Cardiac function, as determined by FS or EF using echocardiography, was similar between the groups at baseline ($p = 0.162$ and $p = 0.15$, respectively). Induction of MI resulted in a similar reduction in FS and EF (6% and 8%, respectively), which was not different between both groups of ligated mice ($p = 0.7$), but differed from sham-operated mice ($p < 0.05$) in the first 24 hours. However, by day 28, FS and EF had returned to baseline in the ligated $Mstn^{-/-}$ mice, an effect not seen in WT counterparts ($p < 0.05$ and $p < 0.01$ respectively) (Figure 3).

Immunohistochemistry and Immunofluorescence

The size of cardiomyocytes was increased in the absence of myostatin as measured by both the cross-sectional area and the minimal Feret's diameter ($p < 0.05$) (Figure 4A). Induction of MI did not alter the size of cardiomyocytes within the groups ($p = 0.2$). Microscopically, there was an obvious disarray of myocardial fibres and cellular infiltration in the MI-induced mice (Figure 4E), whilst the integrity was preserved in sham-operated mice.

Post-MI mice demonstrated an increase in the labelling fraction of BrdU at day 28 post-surgery compared with sham-operated groups ($p < 0.01$) (Figure 4B). There was no difference in the number of BrdU-positive nuclei between the WT and $Mstn^{-/-}$ ligated mice.

$Mstn^{-/-}$ mice had less collagen deposition and a greater amount of viable myocardium in the border region of the infarcted area compared with WT mice ($p < 0.05$) (Figure 4C, F). Similarly, the intensity of immunofluorescence of α-SMA

Please cite this article in press as: Lim S, et al. Absence of Myostatin Improves Cardiac Function Following Myocardial Infarction. Heart, Lung and Circulation (2017), http://dx.doi.org/10.1016/j.hlc.2017.05.138

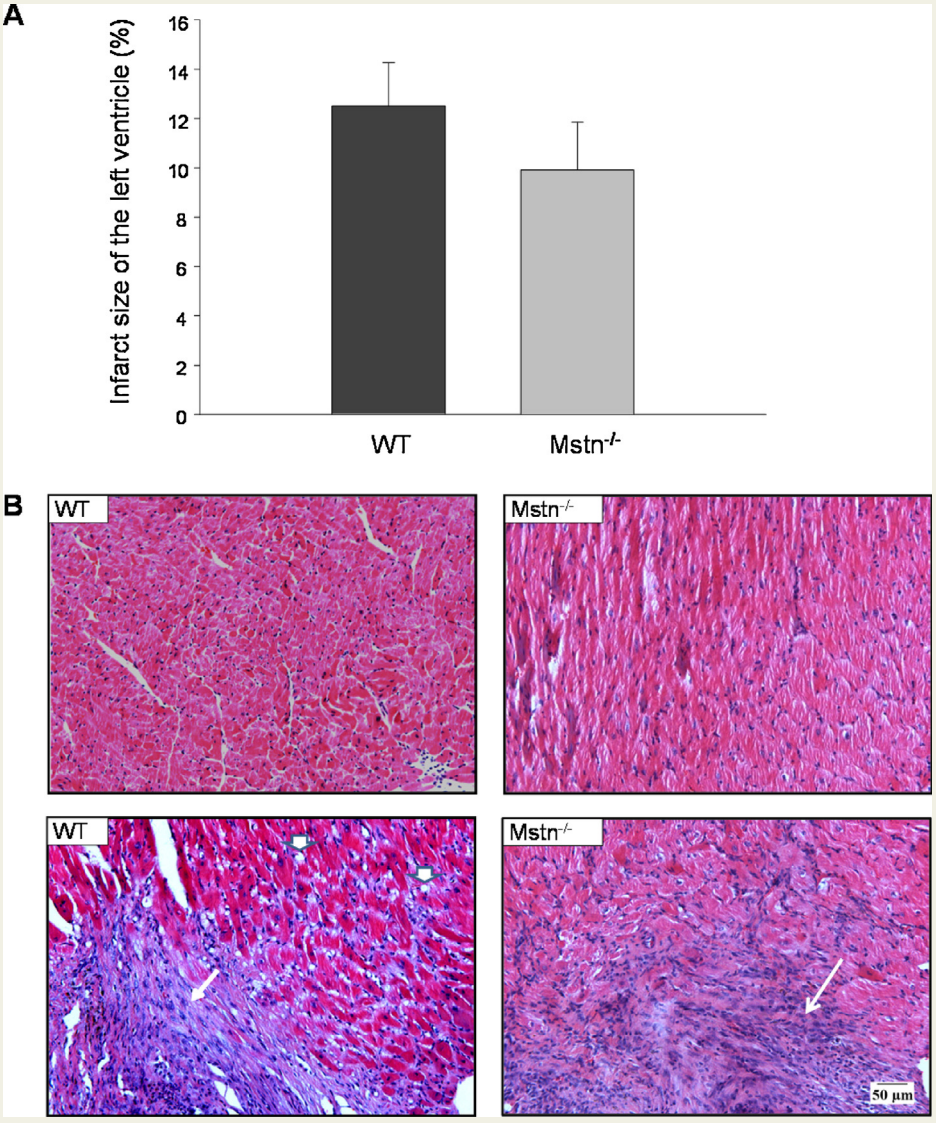

Figure 1 Size of the infarct in the left ventricle. (A) Percentage of infarct size between WT and Mstn$^{-/-}$ mice at day 28 post-MI (mean ± SEM). (B) Representative sections of sham-operated (upper panels) and MI (lower panels) animal. The increased in inflammatory infiltrates were present in the infarcted region of both WT and Mstn$^{-/-}$ mice (arrows) (H&E stain, ×200).

(a marker of myofibroblasts), was increased in the MI groups compared to sham-operated controls, and was restricted to the infarcted zone ($p < 0.001$). Immunofluorescence of α-SMA in the ligated Mstn$^{-/-}$ mice tended to be lower compared with WT ligated mice, although statistical significance was not achieved ($p = 0.15$) (Figure 4D, G).

The Reduction in Fibrosis is Not a Result of an Alteration in Apoptosis, Programmed Necrosis or Cellular Survival

The intensity of immunostaining for anti-PARP-1 (Figure 5A, D) and cleaved caspase-3 (Figure 5B, E) in the peri-infarct region was not different between Mstn$^{-/-}$ and WT mice, but was absent in the sham-operated mice. In contrast, pAkt^{t308} and pAkt^{s473} were present in all four groups of mice, with a greater intensity of immunostaining for the expression of pAkt^{t308} observed in the peri-infarct region of ligated mice, compared to sham-operated controls, irrespective of genotype ($p < 0.05$) (Figure 5C, F)

Discussion

This study demonstrated that the absence of myostatin is associated with (1) a potentially favourable survival outcome post-MI; (2) greater recovery of left ventricular function post-MI; and (3) a reduction in the extent of cardiac fibrosis.

The reduced mortality in the Mstn$^{-/-}$ mice post-MI was unanticipated and, to our knowledge, has not previously been reported. The mortality rate of 20% in WT observed here is consistent with those reported in the literature [15–17]. All deaths except one occurred early post-MI, suggesting the

Please cite this article in press as: Lim S, et al. Absence of Myostatin Improves Cardiac Function Following Myocardial Infarction. Heart, Lung and Circulation (2017), http://dx.doi.org/10.1016/j.hlc.2017.05.138

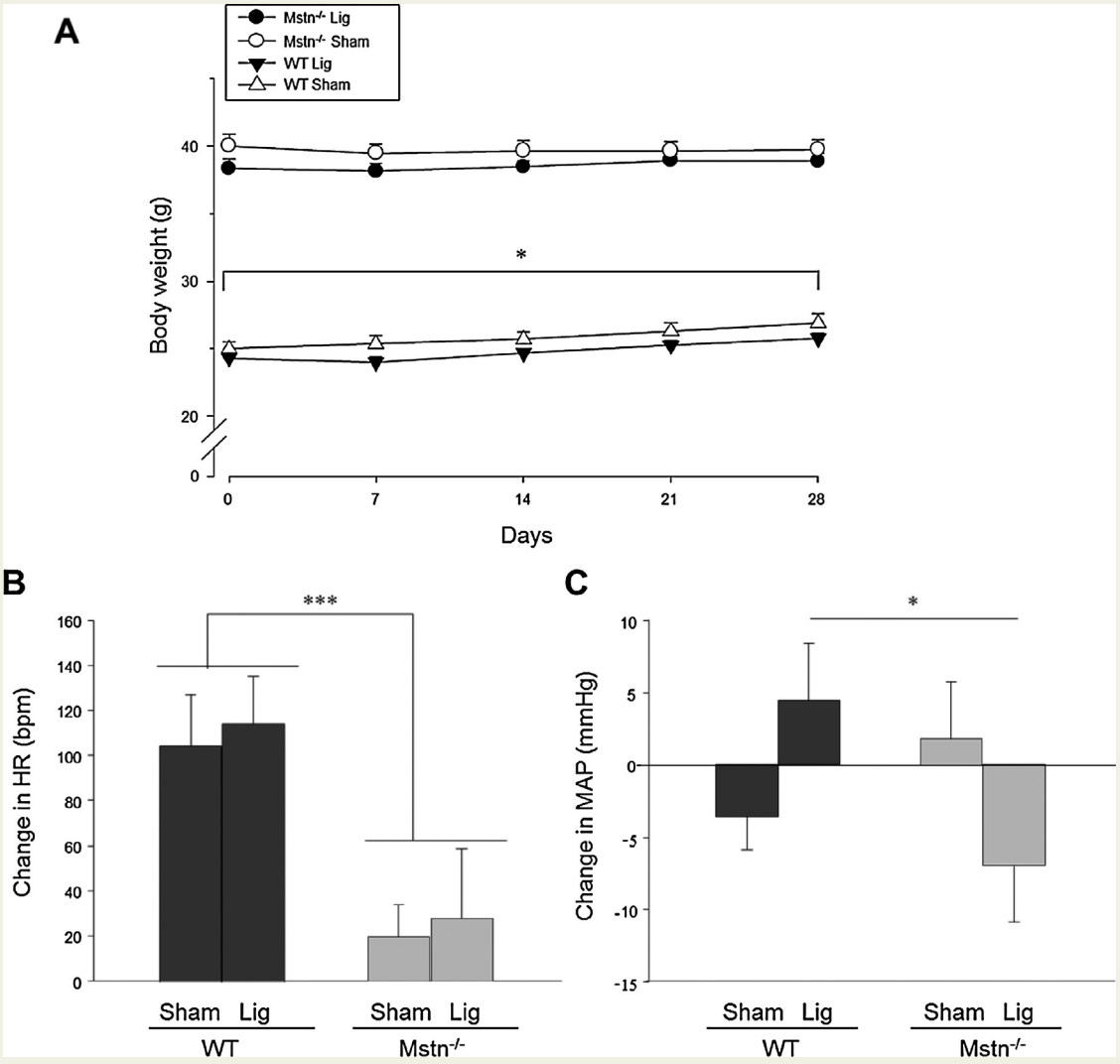

Figure 2 Clinical parameters between WT and Mstn$^{-/-}$ mice. (A) Mean body weight (±SEM). Significant difference was observed in WT mice at baseline and day 28 post-surgery irrespective of surgical procedures, whilst no difference was noted in Mstn$^{-/-}$ mice; (B) Heart rate; (C) Mean arterial pressure (MAP) (mean ±SEM) * $p < 0.05$, ** $p < 0.01$, *** $p < 0.001$.

susceptibility of death in WT mice to open thoracic surgery in general. The cause of death was not apparent at autopsy. The reason for the observed reduction in mortality in Mstn$^{-/-}$ mice is unknown. All procedures were standardised, performed in a random order, with similar operating time between the genotypes, and in the surviving cohort, the reduction in ventricular function and infarct size were similar. Therefore, the difference in mortality is unlikely a result of bias in the surgical procedure. Unfortunately, monitoring of electrocardiograms was not available to determine whether a fatal dysrhythmia had occurred either during or after the procedure.

It is widely recognised that the increased size in Mstn$^{-/-}$ mice is a result of an increase in lean body mass and reduced body fat [18,19], without cardiac hypertrophy [20]. The stability of mean body weight in Mstn$^{-/-}$ mice supports the observation that cachexia has not occurred throughout the study period. Conversely, the increase in body weight in WT mice post-MI, as also previously reported [21] may be due to alterations in fat or lean mass, or extracellular fluid such as water and salt retention.

Open chest surgery alone has been reported to result in haemodynamic changes in WT mice [13]. A postoperative resting tachycardia developed in WT mice, both in the sham and ligated groups. In contrast, maintenance of a physiological HR post-surgery in Mstn$^{-/-}$ mice may imply an altered compensatory mechanism to injury. It is unknown if myostatin affects the autonomic nervous system (ANS), a key determinant of HR. Treatment with carvedilol in rats with an aorto-caval shunt has been shown to inhibit the up-regulation of myostatin mRNA induced by the shunt [2]. This suggests a role of myostatin in the regulation of the ANS.

We have demonstrated, similar to Rodgers et al., that both the LVESD and LVEDD were greater in Mstn$^{-/-}$ mice and remained unchanged at the different time points measured [22]. These data extend previous observations that cardiac

Please cite this article in press as: Lim S, et al. Absence of Myostatin Improves Cardiac Function Following Myocardial Infarction. Heart, Lung and Circulation (2017), http://dx.doi.org/10.1016/j.hlc.2017.05.138

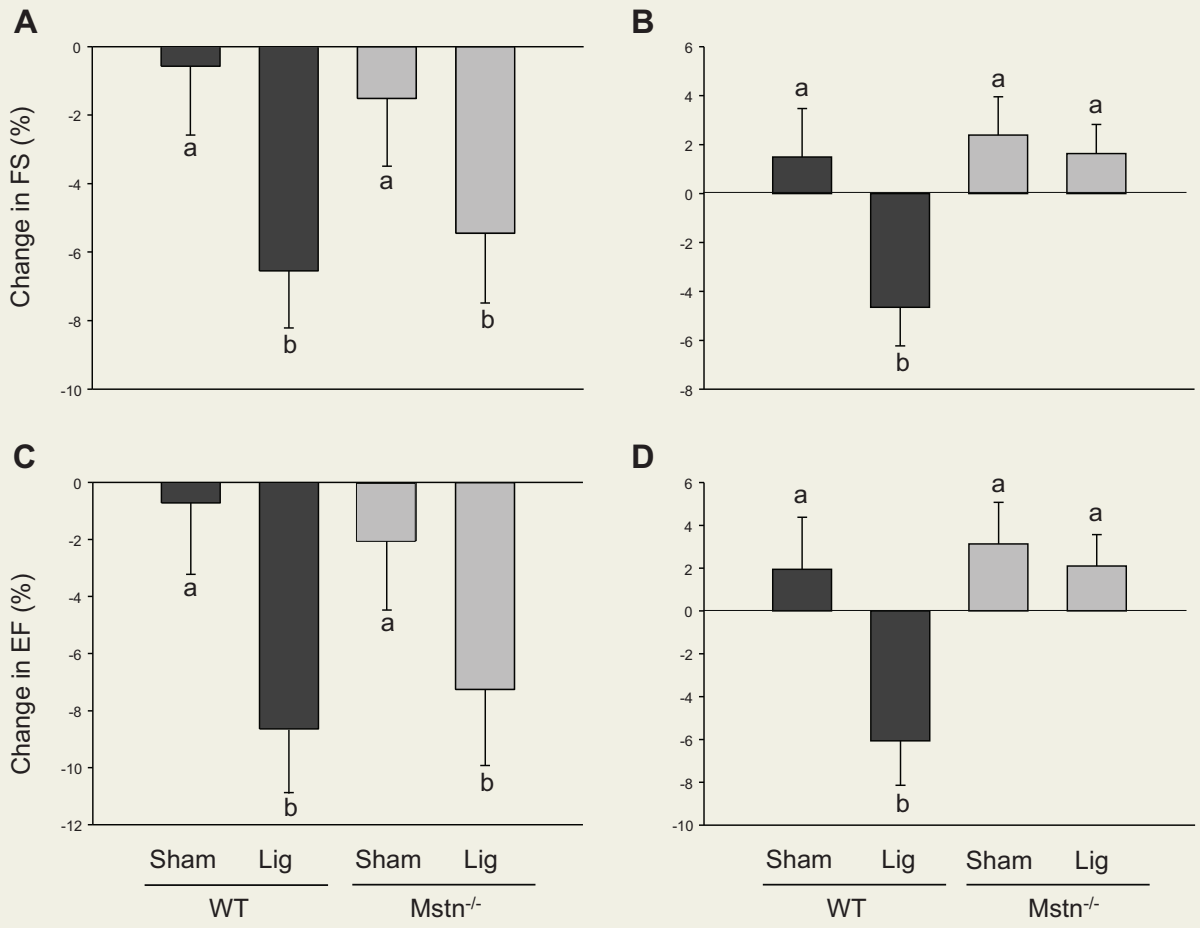

Figure 3 Changes in cardiac function as measured by fractional shortening (FS) from baseline to day one (A) and day 28 (B), and changes in ejection fraction (EF) from baseline to day one (C) and day 28 (D). As expected, significant reduction in cardiac function was observed in ligated mice in both groups (A) and (C). Recovery of cardiac function was observed in all groups, except in MI-induced WT mice (lig). Different letters denote a significant difference $p < 0.05$.

performance is preserved not only following chemical stress [22], but also in the failing heart. This further supports the hypothesis that an eccentric hypertrophy of the myocardium exists in the Mstn$^{-/-}$ mice and the greater LVESD and LVEDD and functional improvement to be consistent with a physiological, and not pathological effect [22].

To investigate the potential mechanism(s) for this apparent protective effect, we assessed the excised hearts histologically. Mstn$^{-/-}$ mice had less scar tissue and more viable myocardium in the border region of the infarcted area compared with WT mice. Excessive collagen deposition has been demonstrated to adversely affect the process of myocardial remodelling [23]. It is widely accepted that cardiac fibroblasts, specifically myofibroblasts, are critical for the maintenance of homeostasis of the extracellular matrix [23] by promoting excessive collagen deposition and/or inhibiting degradation at the site of the infarct through various cytokines and growth factors, one of which is TGF-β [24]. This study suggests that lack of myostatin also resulted in a reduction in cardiac fibrosis, an effect consistent with the reported function of other members of the TGF-β superfamily. Emerging evidence has shown that myostatin is pro-fibrotic in skeletal muscle [6,25]. The proposed mechanisms include a direct stimulation of the proliferation of fibroblasts and expression of extracellular matrix proteins by myostatin [6], a switch to a fibrotic synthetic phenotype to aid in the progression of fibrosis [26], and an enhanced differentiation of fibroblasts to myofibroblasts [25]. A co-stimulatory relationship exists between TGF-β1 and myostatin in promoting the formation of fibrosis [25]. Here, we demonstrate that the activity of α-SMA is induced in the infarcted cardiac tissue, and the intensity of α-SMA activity is lower in Mstn$^{-/-}$ mice, compared with WT mice post-MI, suggesting less myofibroblasts in the Mstn$^{-/-}$ mice. One possible mechanism is that the absence of myostatin reduces the formation of fibrosis in the myocardium and likely does so by preventing/reducing the differentiation of fibroblasts to myofibroblasts, an effect previously reported in skeletal muscle fibroblasts [25].

Several studies have reported conflicting results between cardiac fibrosis and myostatin [20,27]. Morissette and colleagues reported a reduction in cardiac fibrosis in senescent

Please cite this article in press as: Lim S, et al. Absence of Myostatin Improves Cardiac Function Following Myocardial Infarction. Heart, Lung and Circulation (2017), http://dx.doi.org/10.1016/j.hlc.2017.05.138

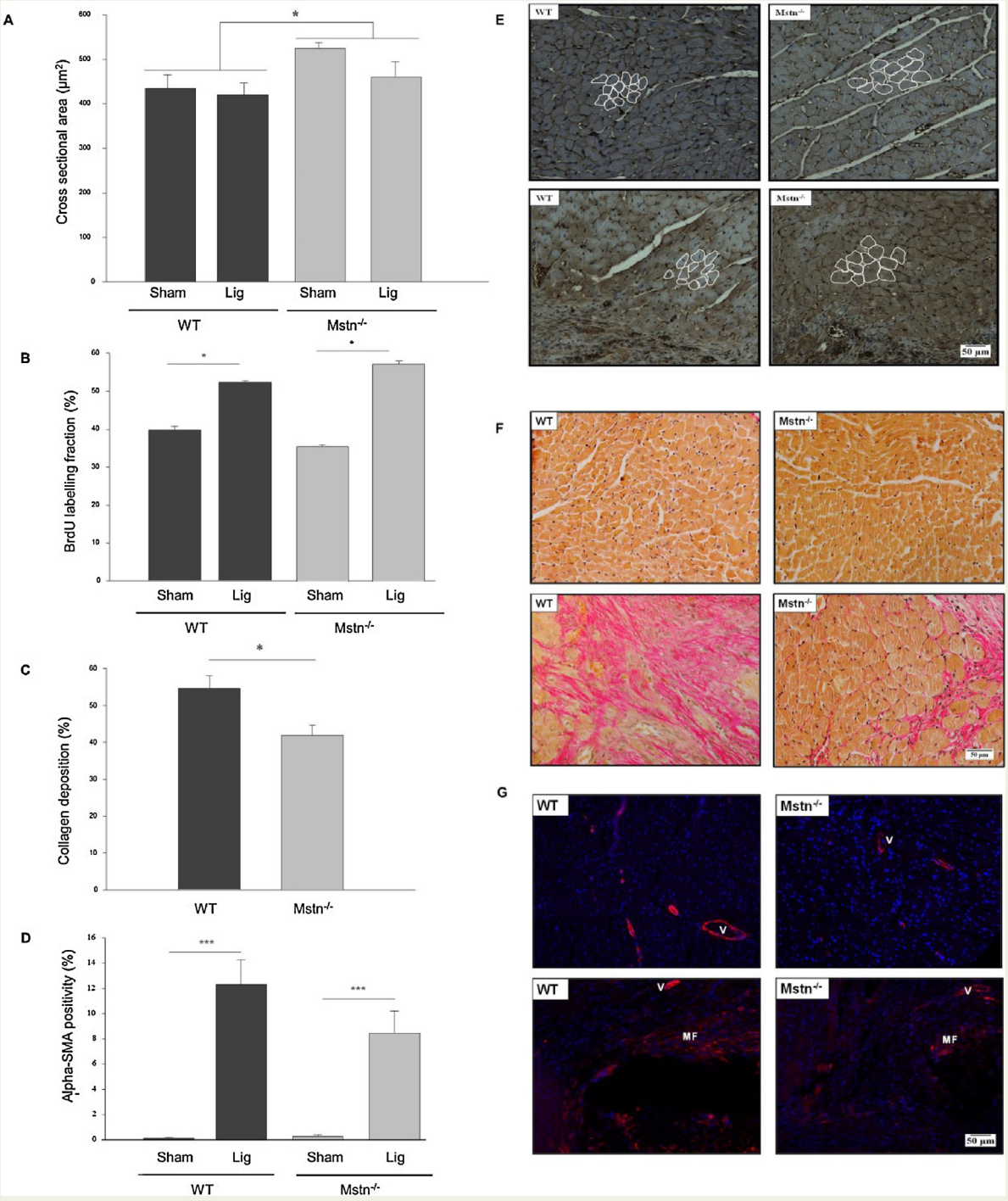

Figure 4 Immunohistochemistry and immunofluorescence. (A) Size of the cardiomyocytes by cross-sectional area. (B) Percentage of BrdU positive nuclei (BrdU labelling fraction) in the border region of the infarcted ventricle. (C) Percentage of collagen deposition in the infarcted region relative to the peri-infarct area between Mstn$^{-/-}$ and WT mice. (D) Percentage of cells expressing alpha-smooth muscle actin (α-SMA) immunofluorescence (mean ± SEM) (* $p < 0.05$, ** $p < 0.01$, *** $p < 0.001$). Representative sections of the myocardium in sham-operated (upper panels) and MI (lower panels) stained with (E) laminin, (F) Van Gieson and (G) α-SMA immunofluorescence antibody. V: blood vessel, MF: myofibroblasts.

Mstn$^{-/-}$ mice compared with WT mice, but a mechanism was not proposed [27]. Cohn and co-workers demonstrated that myostatin does not regulate cardiac hypertrophy or fibrosis in the double mutant *mdx*/Mstn$^{-/-}$ mice compared with *mdx* mice [20]. However, the mean body weights between Mstn$^{-/-}$ and WT mice in that study were similar (40.3 ± 2.1 g vs 37.4 ± 0.9 g) which may explained the lack of difference between the size of cardiomyocytes and heart

Please cite this article in press as: Lim S, et al. Absence of Myostatin Improves Cardiac Function Following Myocardial Infarction. Heart, Lung and Circulation (2017), http://dx.doi.org/10.1016/j.hlc.2017.05.138

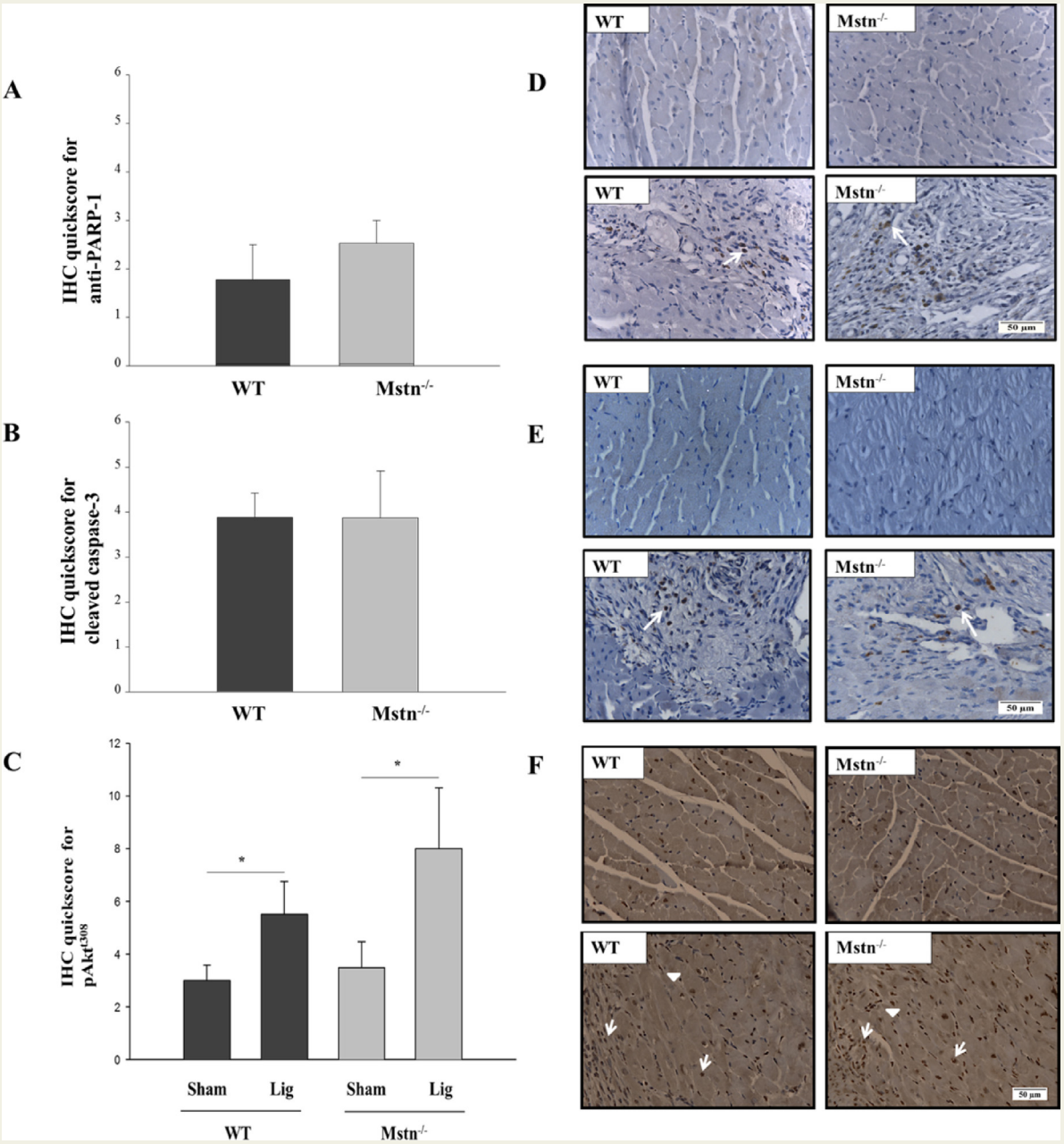

Figure 5 Semiquantitative IHC of (A) anti-PARP-1 antibody, (B) anti-cleaved caspase-3 antibody, (C) pAKT^{308} antibody (* $p < 0.05$) in the peri-infarct region of the WT and Mstn$^{-/-}$ mice post-MI. Representative section of cardiac tissue in sham-operated (upper panels) and MI-induced (lower panels) mice for (D) anti-PARP-1 antibody, (E) cleaved caspase-3 antibody, and (F) pAKT^{308} antibody. Sections counterstained with haematoxylin to visualise the nuclei (arrow heads). DAB-positive cells (arrows) were present in MI groups but not sham animals (×400).

weights. In addition, the assessment of collagen deposition reported by Cohn et al. was performed without stimulation. It is also possible that the severe cardiomyopathic changes in *mdx* mice circumvented the effects of the absence of myostatin in the heart and thereby, negated any possible benefit that knockout of myostatin imparts.

To determine if the restoration in cardiac function in Mstn$^{-/-}$ mice may be a result of other mechanism(s), we examined the size of cardiomyocytes, DNA synthesis, and alteration in cellular growth and apoptotic pathways. While the size of cardiomyocytes was greater in the absence of myostatin, induction of MI did not increase the size of cardiomyocytes further. This supports the earlier observation that the increase in heart weight pre-MI is likely due to the increase in the number and size of cardiomyocytes. However, the increase in function in the hearts of Mstn$^{-/-}$ mice post-MI is not the result of pathological hypertrophy. There was no difference in the number of newly synthesised cells in the myocardium between the groups following MI. Although the characteristics of the newly synthesised cells were not

Please cite this article in press as: Lim S, et al. Absence of Myostatin Improves Cardiac Function Following Myocardial Infarction. Heart, Lung and Circulation (2017), http://dx.doi.org/10.1016/j.hlc.2017.05.138

examined in this study, the distribution of the cells indicated the likely candidates were non-cardiomyocytes. This observation is supported at least in part, by the *in vitro* studies by Morissette et al. which demonstrated that myostatin regulates the growth of cultured neonatal cardiomyocytes but does not affect the number of cardiomyocytes [28]. We noted no difference in apoptosis and programmed necrosis, which is unsurprising, given that apoptosis and necrosis of cardiomyocytes tend to occur early following a cardiac injury [29]. It is however possible that other pathways or enzymes (eg. intracellular Ca^{2+} concentrations, caspase 8 etc.) are involved which were not examined. Similarly, we observed a greater intensity of immunostaining for the growth and survival factor $pAkt^{t308}$ in ligated animals with no difference observed between $Mstn^{-/-}$ and WT mice. Collectively, these data suggest that while cellular survival may be important in the early remodelling process, it is less critical at 28 days post-MI when the formation of scar tissue and fibrosis becomes a more prominent feature.

In summary, the absence of myostatin appears to protect cardiac function following an acute MI. The mechanism may relate to a reduction in the extent of fibrosis. This study suggests that absence of myostatin may be potentially beneficial to the heart post-MI. Further studies in this area are warranted to assess whether an antagonist to myostatin may be beneficial in preserving cardiac function following an acute MI.

Funding

This work was supported by a Research fellowship from the Sarah Fitzgibbon Trust, the Cardiology Research Charitable Trust, the Waikato Medical Research Foundation, the Australasian College of Physicians General Endowment Fund, and the National Heart Foundation, New Zealand.

Conflict of Interest

None.

Acknowledgements

We thank Mr Ric Broadhurst, Mr Robert Smith, Ms Genevie Sheriff at the Small Animal Colony unit at AgResearch for looking after the animals. We also thank Mr Harold Henderson for Biometric analysis and presentation of data.

References

[1] McPherron AC, Lawler AM, Lee SJ. Regulation of skeletal muscle mass in mice by a new TGF-beta superfamily member. Nature 1997;387:83–90.
[2] Shyu KG, Lu MJ, Wang BW, Sun HY, Chang H. Myostatin expression in ventricular myocardium in a rat model of volume-overload heart failure. Eur J Clin Invest 2006;36:713–9.
[3] George I, Bish LT, Kamalakkannan G, Petrilli CM, Oz MC, Naka Y, et al. Myostatin activation in patients with advanced heart failure and after mechanical unloading. Eur J Heart Fail 2010;12:444–53.
[4] Gruson D, Ahn SA, Ketelslegers JM, Rousseau MF. Increased plasma myostatin in heart failure. Eur J Heart Fail 2011;13:734–6.
[5] Lenk K, Erbs S, Hollriegel R, Beck E, Linke A, Gielen S, et al. Exercise training leads to a reduction of elevated myostatin levels in patients with chronic heart failure. Eur J Prev Cardiol 2011;19:404–11.
[6] Li ZB, Kollias HD, Wagner KR. Myostatin directly regulates skeletal muscle fibrosis. J Biol Chem 2008;283:19371–8.
[7] Li ZB, Zhang J, Wagner KR. Inhibition of myostatin reverses muscle fibrosis through apoptosis. J Cell Sci 2012;125:3957–65.
[8] Biesemann N, Mendler L, Kostin S, Wietelmann A, Borchardt T, Braun T. Myostatin induces interstitial fibrosis in the heart via TAK1 and p38. Cell Tissue Res 2015;361(3):779–87.
[9] Ellmers LJ, Scott NJ, Medicherla S, Pilbrow AP, Bridgman PG, Yandle TG, et al. Transforming growth factor-beta blockade down-regulates the renin-angiotensin system and modifies cardiac remodeling after myocardial infarction. Endocrinology 2008;149:5828–34.
[10] Anderson B. Echocardiography - the normal examination and echocardiographic measurements. Australia: MGA Graphics; 2000.
[11] Takagawa J, Zhang Y, Wong ML, Sievers RE, Kapasi NK, Wang Y, et al. Myocardial infarct size measurement in the mouse chronic infarction model: comparison of area- and length-based approaches. J Appl Physiol 2007;102:2104–11.
[12] Kitamura M, Shimizu M, Kita Y, Yoshio H, Ino H, Misawa K, et al. Quantitative evaluation of the rate of myocardial interstitial fibrosis using a personal computer. Jpn Circ J 1997;61:781–6.
[13] Lutgens E, Daemen MJ, de Muinck ED, Debets J, Leenders P, Smits JF. Chronic myocardial infarction in the mouse: cardiac structural and functional changes. Cardiovasc Res 1999;41:586–93.
[14] Detre S, Saclani Jotti G, Dowsett MA. A "quickscore" method for immunohistochemical semiquantitation: validation for oestrogen receptor in breast carcinomas. J Clin Pathol 1995;48:876–8.
[15] Michael LH, Ballantyne CM, Zachariah JP, Gould KE, Pocius JS, Taffet GE, et al. Myocardial infarction and remodeling in mice: effect of reperfusion. Am J Physiol 1999;277:H660–8.
[16] Salto-Tellez M, Yung Lim S, El-Oakley RM, Tang TP, ALmsherqi ZA, Lim SK. Myocardial infarction in the C57BL/6J mouse: a quantifiable and highly reproducible experimental model. Cardiovasc Pathol: the official journal of the Society for Cardiovascular Pathology 2004;13:91–7.
[17] Ahn D, Cheng L, Moon C, Spurgeon H, Lakatta EG, Talan MI. Induction of myocardial infarcts of a predictable size and location by branch pattern probability-assisted coronary ligation in C57BL/6 mice. Am J Physiol Heart Circ Physiol 2004;286:H1201–7.
[18] McPherron AC, Lee SJ. Double muscling in cattle due to mutations in the myostatin gene. Proceedings of the National Academy of Sciences of the United States of America 1997;94:12457–61.
[19] McPherron AC, Lee SJ. Suppression of body fat accumulation in myostatin-deficient mice. J Clin Invest 2002;109:595–601.
[20] Cohn RD, Liang HY, Shetty R, Abraham T, Wagner KR. Myostatin does not regulate cardiac hypertrophy or fibrosis. Neuromuscular Disord: NMD 2007;17:290–6.
[21] Gould KE, Taffet GE, Michael LH, Christie RM, Konkol DL, Pocius JS, et al. Heart failure and greater infarct expansion in middle-aged mice: a relevant model for postinfarction failure. Am J Physiol Heart Circ Physiol 2002;282:H615–21.
[22] Rodgers BD, Interlichia JP, Garikipati DK, Mamidi R, Chandra M, Nelson OL, et al. Myostatin represses physiological hypertrophy of the heart and excitation-contraction couping. J Physiol 2009;587:4873–86.
[23] Camelliti P, Borg TK, Kohl P. Structural and functional characterisation of cardiac fibroblasts. Cardiovasc Res 2005;65:40–51.
[24] Souders CA, Bowers SL, Baudino TA. Cardiac fibroblast: the renaissance cell. Circ Res 2009;105:1164–76.
[25] Zhu J, Li Y, Shen W, Qiao C, Ambrosio F, Lavasani M, et al. Relationships between transforming growth factor-beta1, myostatin, and decorin: implications for skeletal muscle fibrosis. J Biol Chem 2007;282:25852–63.
[26] Artaza JN, Singh R, Ferrini MG, Braga M, Tsao J, Gonzalez-Cadavid NF. Myostatin promotes a fibrotic phenotypic switch in multipotent C3H 10T1/2 cells without affecting their differentiation into myofibroblasts. J Endocrinol 2008;196:235–49.
[27] Morissette MR, Stricker JC, Rosenberg MA, Buranasombati C, Levitan EB, Mittleman MA, et al. Effects of myostatin deletion in aging mice. Aging Cell 2009;8:573–83.
[28] Morissette MR, Cook SA, Foo S, McKoy G, Ashida N, Novikov M, et al. Myostatin regulates cardiomyocyte growth through modulation of Akt signaling. Circ Res 2006;99:15–24.
[29] Fraccarollo D, Galuppo P, Bauersachs J. Novel therapeutic approaches to post-infarction remodelling. Cardiovasc Res 2012;94:293–303.

Please cite this article in press as: Lim S, et al. Absence of Myostatin Improves Cardiac Function Following Myocardial Infarction. Heart, Lung and Circulation (2017), http://dx.doi.org/10.1016/j.hlc.2017.05.138